Topological Protection of Supercontinuum Generation

Chaoxiang Xi, Zhen Jiang, Lefeng Zhou, and Guangqiang He*
State Key Laboratory of Advanced Optical Communication Systems and Networks, Shanghai Jiao Tong University, Shanghai, 200240, China
**Corresponding author: gqhe@sjtu.edu.cn*

Abstract: We demonstrate a topologically protected supercontinuum generation process based on lithium niobate valley photonic crystals. Simulation results show that this structure can achieve full coverage topological protection of the supercontinuum spectrum.

1. Introduction

Topological photonics has grown rapidly in recent years, and it offers the possibility of topological protection for the transmission of both classical and quantum waves. Topologically protected edge states have excellent properties such as defect resistance and unidirectional transport, which allows optical processes insensitive to structural defects. Topological features can provide robustness for the transport of two-photon states [1], quantum entangled states [2,3], topological insulator lasers [4], which can be applied to many frontiers.

Here we present a topologically protected supercontinuum generation (SCG) scheme. The valley kink states propagating along the topological interface are observed in valley photonic crystals (VPCs), which reveals the quantum valley hall (QVH) effect. We simulated the dispersion relation of this topological waveguide and calculated its SCG process under picosecond pulse pumping conditions.

2. Topological waveguide

Topological valley kink states in topological waveguides have single-mode and linear-dispersion properties, providing a practical platform for optical nonlinear effects. Here we propose a z-cut lithium niobate (LN) topological waveguide for SCG with the structure shown in Fig. 1. In Fig. 1(a), the design resembles a graphene-like lattice consisting of equilateral triangular nanoholes possessing C_6 symmetry with lattice constant a = 540 nm. Side lengths of nanoholes are defined as d_1 and d_2, where $d_1 = 0.25a$ and $d_2 = 0.75a$. Topological valley kink states are supported at the interface of VPC_1 and VPC_2. Fig. 1(b) shows the calculated dispersion at the interface. The green line and the blue dots represent the dispersion of topological edge states and projected bulk states, respectively. The yellow area indicates the topological bandgap (~15.1THz) from 183.6THz to 198.7THz. The propagation directions of kink states within the bandgap are locked to two different valleys owing to the QVH effect. Therefore, edge states within the topological bandgap are topologically protected. The simulation result of the field distribution (at 1560nm) when VPC_1 and VPC_2 have a "Z" shaped interface is shown in Fig. 1(c), indicating the topological protection characteristics.

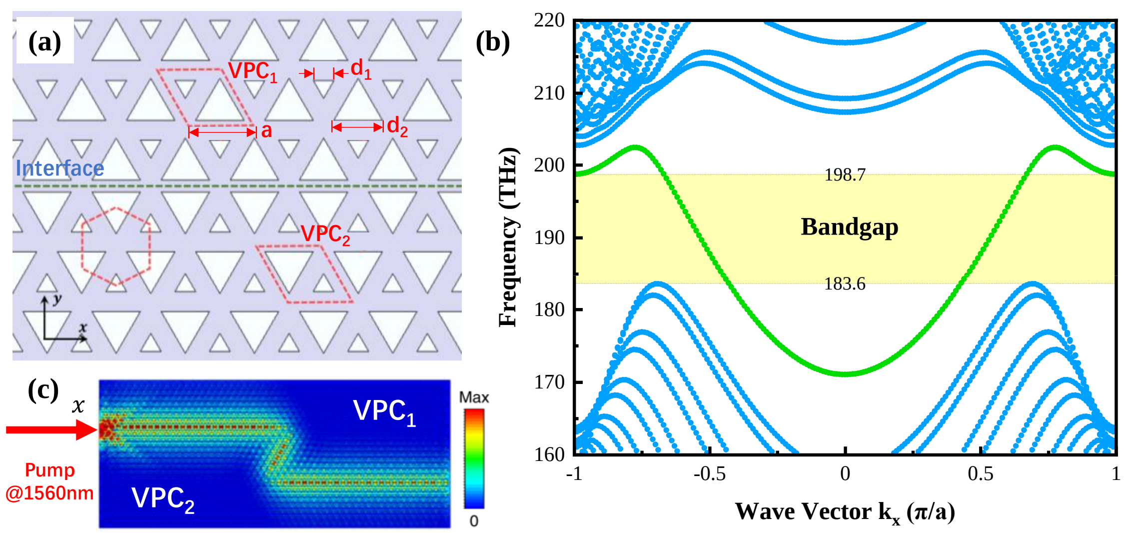

Fig. 1. Topological waveguide. (a) Structure of the valley photonic crystal. (b) Dispersion of topological valley kink states at the interface. (c) Simulated field distribution in the VPC at 1560nm.

3. Supercontinuum Generation

Supercontinuum generation, a spectral broadening phenomenon, occurs when ultrashort intense pulses propagate through a nonlinear material. We use MATLAB to simulate topologically protected SCG, which can achieve the SCG while maintaining the topological properties. In the simulation, we send pulses from a picosecond optical parametric oscillator centered at 1560 nm with a 100-MHz repetition rate into a 50-mm z-cut LN topological waveguide. The pulse width is 2 ps and the pulse energy is 500 pJ. The effective mode area (A_{eff}) is 1 μm^2. The nonlinear index (n_2) of LN is 2×10^{-19}m^2/W [5]. The propagation loss of the LN topological waveguide is 0.16 dB/cm. Due to the limited operating bandwidth of the topological valley kink states, the second harmonic generation (SHG) caused by the second-order nonlinear coefficient of LN is not considered.

The spectral and temporal pulse evolution in the topological waveguide are shown in Fig. 2(a) and (b). It is evident that by the time the pulse propagates to ~20 mm of the topological waveguide, the spectrum of the pulse has broadened significantly. The time-domain evolution demonstrates the generation of dispersive waves (DWs). When the pulse propagates to 20.5mm and 50mm, the spectra are drawn in Fig. 2(c). At the same time, the vast majority of SCG spectral components are still within the topological bandgap (183.6-198.7THz) and maintain topological protection properties. Fig. 2(d) plots the performance of the dispersion operator D (sum of Taylor series n-th terms, $n\geqslant2$), and the purple arrow marks the zero-crossing point. The zero-crossing point of the dispersion operator is used to predict the spectral position where DW occurs, which is consistent with the spectrum in Fig. 2(c).

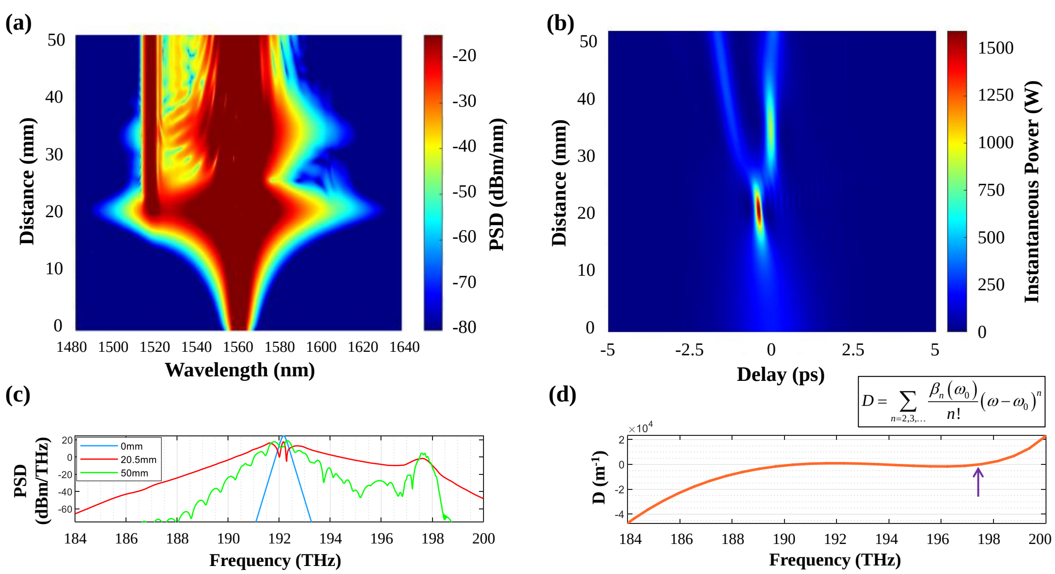

Fig. 2. Simulation results. (a), (b) Spectral and temporal pulse evolution as a function of propagation distance in the topological waveguide. (c) Spectra at input (blue curve), 20.5 mm (red curve), and output (green curve). (d) Dispersion operator D for a pump centered at 1560 nm. β_n corresponds to the n-th order dispersion coefficient, and ω_0 is the pump frequency.

4. Conclusion

Topological photonics has made a big splash in nonlinear optics. We innovatively propose a topologically protected supercontinuum generation process based on lithium niobate valley photonic crystals. By simulating the dispersion and the pulse evolution, we demonstrate a high overlap between the supercontinuum spectrum and the topological protection range (~15.1THz). This idea provides possibilities for novel topological nonlinear optical devices.

The authors acknowledge the support from the Key-Area Research and Development Program of Guangdong Province (Grant 2018B030325002) and the National Natural Science Foundation of China (Grant 62075129).

References

[1] A. Blanco-Redondo, et al. "Topological protection of biphoton states." Science **362**, 568-571 (2018).
[2] K. Tschernig, et al. "Topological protection versus degree of entanglement of two-photon light in photonic topological insulators." Nat. Commun. **12**, 1-8 (2021).
[3] J. Zhen, et al. "Topological protection of continuous frequency entangled biphoton states." Nanophotonics **10**, 4019-4026 (2021).
[4] M. A. Bandres, et al. "Topological insulator laser: Experiments." Science **359**, 1231 (2018).
[5] Y. Okawachi, et al. "Chip-based self-referencing using integrated lithium niobate waveguides." Optica **7**, 702-707 (2020).

CLEO 2022 JTh3B.54

Topological Protection of Supercontinuum Generation

SHANGHAI JIAO TONG UNIVERSITY

STATE KEY LABORATORY OF ADVANCED OPTICAL COMMUNICATION SYSTEMS AND NETWORKS

LABORATORY OF QUANTUM NONLINEAR PHOTONICS

https://qnp.sjtu.edu.cn

Chaoxiang Xi, Zhen Jiang, Lefeng Zhou, and Guangqiang He*

(*gqhe@sjtu.edu.cn)

Abstract

We demonstrate a topologically protected supercontinuum generation process based on lithium niobate valley photonic crystals (VPCs). Simulation results show that this structure can achieve full coverage topological protection of the supercontinuum spectrum.

1. Introduction

Topological photonics has grown rapidly in recent years, and it offers the possibility of topological protection for the transmission of both classical and quantum waves. Topologically protected edge states have excellent properties such as defect resistance and unidirectional transport, which allows optical processes insensitive to structural defects. Topological features can provide robustness for the transport of biphoton states [1], quantum entangled states [2, 3], topological insulator lasers [4], which can be applied to many frontiers.

2. Topological Waveguide

Here we propose a z-cut lithium niobate (LN) topological waveguide for SCG with the structure shown in Fig. 1. The lattice constant a = 540 nm. Side lengths of nanoholes d_1 = 0.25a and d_2 = 0.75a. Topological valley kink states are supported at the interface of VPC_1 and VPC_2. Fig. 1(b) shows the calculated dispersion at the interface. The yellow area indicates the topological bandgap (~15.1 THz) from 183.6 THz to 198.7 THz. The simulation result of the field distribution (at 1560 nm) when VPC_1 and VPC_2 have a "Z" shaped interface is shown in Fig. 1(c), indicating the topological protection characteristics.

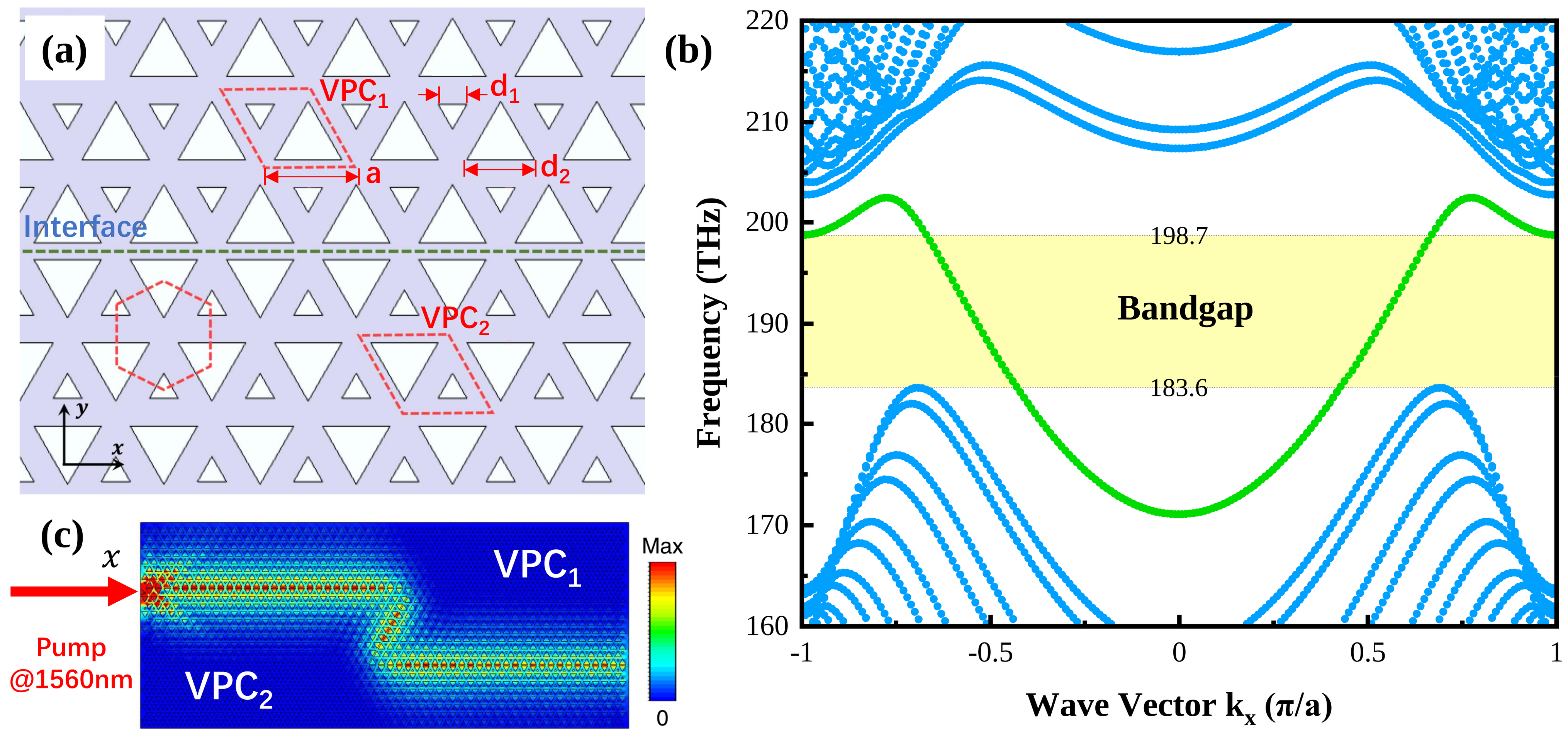

Fig. 1 Topological Waveguide

3. Topologically Protected Supercontinuum Generation (SCG)

In the MATLAB simulation, we send pulses from a picosecond optical parametric oscillator centered at 1560 nm with a 100-MHz repetition rate into a 50-mm z-cut LN topological waveguide. The pulse width is 2 ps and the pulse energy is 500 pJ. The effective mode area (A_{eff}) is 1 μm^2. The nonlinear index (n_2) of LN is 2×10^{-19} m^2/W [5]. The propagation loss of the LN topological waveguide is 0.16 dB/cm. Due to the limited bandgap, the second harmonic generation (SHG) is not considered.

The spectral and temporal pulse evolution in the topological waveguide are shown in Fig. 2(a) and (b). The time-domain evolution demonstrates the generation of dispersive waves (DWs). When the pulse propagates to 20.5 mm and 50 mm, the spectra are drawn in Fig. 2(c). At the same time, the vast majority of SCG spectral components are still within the topological bandgap (183.6-198.7 THz). Fig. 2(d) plots the performance of the dispersion operator D (sum of Taylor series n-th terms, n≥2), and the purple arrow marks the zero-crossing point. The zero-crossing point of the dispersion operator is used to predict the spectral position where DW occurs, which is consistent with the spectrum in Fig. 2(c).

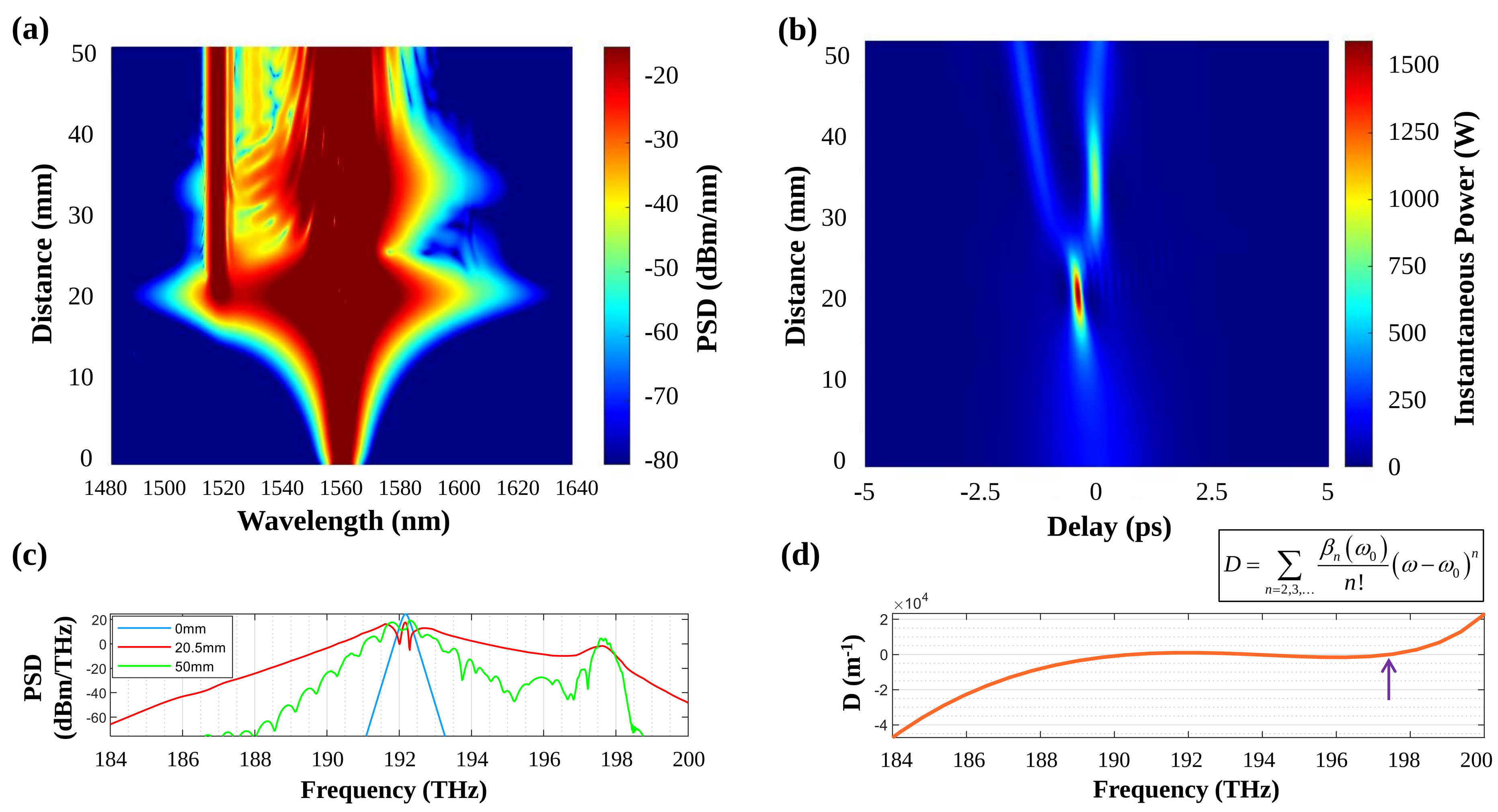

Fig. 2 Simulation Results

References

[1] A. Blanco-Redondo, et al. "Topological protection of biphoton states." Science **362**, 568-571 (2018).

[2] K. Tschernig, et al. "Topological protection versus degree of entanglement of two-photon light in photonic topological insulators." Nat. Commun. **12**, 1-8 (2021).

[3] J. Zhen, et al. "Topological protection of continuous frequency entangled biphoton states." Nanophotonics **10**, 4019-4026 (2021).

[4] M. A. Bandres, et al. "Topological insulator laser: Experiments." Science **359**, 1231 (2018).

[5] Y. Okawachi, et al. "Chip-based self-referencing using integrated lithium niobate waveguides." Optica **7**, 702-707 (2020).